Stabilization and "Debundling" of Single-Wall Carbon Nanotube Dispersions in *N*-Methyl-2-pyrrolidone (NMP) by Polyvinylpyrrolidone (PVP)

Tawfique Hasan, Vittorio Scardaci, PingHeng Tan, Aleksey G. Rozhin, William I. Milne, and Andrea C. Ferrari*

Engineering Department, Cambridge University, 9 JJ Thomson Avenue, Cambridge, United Kingdom

Received: March 22, 2007; In Final Form: May 13, 2007

We present a simple method to stabilize single-wall carbon nanotube (SWNT) dispersions in *N*-methyl-2-pyrrolidone (NMP) by polyvinylpyrrolidone (PVP). A significant population of isolated SWNTs as well as small bundles of SWNTs in NMP is obtained by ultrasonic treatment followed by vacuum filtration through glass fiber filters. The resulting dispersions in pure NMP are monitored by photoluminescence (PL) spectroscopy over a period of 3 weeks. The PL intensities of such dispersions decrease with time, suggesting slow microscopic aggregation of nanotubes. However, addition of PVP dramatically improves the stability. In addition, PVP also spontaneously "debundles" some nanotube aggregates, increasing the isolated SWNT population without further ultrasonic treatment.

1. Introduction

Single-wall carbon nanotubes (SWNTs) tend to form ropes or bundles[1,2] due to strong intertube van der Waals interactions.[3,4] Bundles can aggregate further, forming entangled networks. Heavily entangled and disordered SWNT networks do not have the optimum mechanical, thermal, and electronic properties of individual SWNTs.[5–10] Thus, great effort has been devoted over the years to prepare stable dispersions of SWNTs in different solvents.[11–34] To date, such SWNT dispersions in aqueous media have been reported with the aid of ionic and nonionic surfactants,[11–13] water soluble polymers,[14,15] and DNA.[16] In aqueous media, surfactants form micelles around the SWNTs, preventing reaggregation.[11–13,17] In the case of polymers, wrapping[14,18–20] of nanotube sidewalls is considered to be the mechanism of dispersion. Reports of π-stacking of aromatic rings in the surfactants[13] or polymers[19,21] with the graphitic surface of SWNTs have also been published. In general, polymers can efficiently be used as dispersing agents for SWNTs in both aqueous and nonaqueous media,[14,15,22] whereas the effectiveness of commercially available surfactants is usually limited to the aqueous environment.[11–13,23] The dispersion of chemically modified[24–26] and unmodified[27–34] SWNTs with or without dispersants in different amide solvents has also been extensively investigated. In order to disperse pristine SWNTs directly into amide solvents without significant sidewall and end-cap functionalization, high values of hydrogen bond acceptance basicity and solvochromic parameter and a negligible value of hydrogen bond donation parameter are required.[28,35] Nevertheless, the complete set of criteria for SWNT dispersions into amide solvents is not yet well understood.[30,34]

Among amide solvents, *N*-methyl-2-pyrrolidone (NMP) appears to be one of the most promising[28] with a reported dispersion limit of 0.01–0.02 g/L.[29,34] However, no specific information regarding the stability of such dispersions is available. Polyvinylpyrrolidone (PVP) has already been used to disperse[14,36] or stabilize[12] SWNTs in aqueous environment.

This is speculated to be a thermodynamically driven wrapping process of hydrophobic SWNTs by PVP molecules.[14]

Here we show that simple addition of PVP to ultrasonically treated and vacuum-filtered SWNT dispersions in NMP (SWNT/NMP) can also stabilize them in a nonaqueous environment. More importantly, a significant increase in photoluminescence (PL) intensity without further ultrasonic treatment indicates spontaneous "debundling" of small SWNT aggregates by PVP addition. By comparing the maps obtained by photoluminescence excitation (PLE) spectroscopy, we show that SWNT species with larger diameters "debundle" more readily in the presence of PVP. We also observe that SWNT dispersions in pure NMP with a concentration of ≈0.01 g/L are not thermodynamically stable. Though the SWNT/NMP dispersions remain stable by visual inspection for at least 5 weeks, the PL intensities of the dispersions gradually decrease, indicating slow microscopic aggregations. We also show that nonionic surfactants (Igepal DM-970, Triton X-100, and Pluronic F98) do not stabilize SWNTs in NMP.

2. Experimental Section

We consider four groups of vacuum-filtered dispersions of purified HiPco[37] SWNTs (lot no. PO279; Carbon Nanotechnologies Inc.) in NMP, as summarized in Table 1. In group A, B, and C dispersions, the starting concentration of SWNTs is 0.04 g/L, whereas in group D it is 0.09 g/L. In group D, a higher starting concentration of SWNTs is used to marginally accelerate the SWNT aggregation process so that the effect of PVP on SWNT "debundling" can be clearly seen. According to the data sheet, SWNTs account for ≈80 wt % of the purified HiPco sample. The remaining 20 wt % consists of moisture (≈5 wt %) and metal catalysts (≈15 wt %). We verified this by further thermogravimetric analysis. Therefore, the concentration of SWNTs before ultrasonic treatment excluding the catalysts and moisture is ≈0.03 g/L (80% of 0.04 g/L) in groups A, B, and C and ≈0.07 g/L (80% of 0.09 g/L) in group D. The weight of the samples is measured by a standard microbalance (Fisher Scientific). Instrumental error for the measurements is within ±10%. The SWNTs are dispersed in spectroscopic-grade NMP

* Corresponding author. Phone: +44 1223 7 48351. Fax: +44 1223 7 48348. E-mail: acf26@eng.cam.ac.uk.

Stabilization and "Debundling" of SWNTs in NMP

J. Phys. Chem. C, Vol. 111, No. 34, 2007 **12595**

TABLE 1: Specifications of the Dispersions Used in This Study

group	sample	solvent	filter (μm)	initial SWNT concn (g/L)[a]	final SWNT concn (g/L)[b]	additional information
A	A1	NMP	0.7	0.03	0.0142	Igepal DM-970 used as dispersant
	A2	NMP	0.7	0.03	0.0147	Triton X-100 used as dispersant
	A3	NMP	0.7	0.03	0.0149	Pluronic F98 used as dispersant
B	B1	NMP	0.3	0.03	0.0090	
	B2	NMP	0.5	0.03	0.0098	
	B3	NMP	0.7	0.03	0.0106	
C	C1	NMP	0.7	0.03	0.0106	1.67 g/L PVP added after preparation
	C2	NMP	0.7	0.03	0.0106	3.33 g/L PVP added after preparation
	C3	NMP	0.7	0.03	0.0106	6.67 g/L PVP added after preparation
D	D1	NMP	0.7	0.07	0.0330	PLE map taken just after preparation
	D2	NMP	0.7	0.07	0.0330	PLE map taken after 8 days of preparation
	D3	NMP	0.7	0.07	0.0330	5 g/L PVP added after preparation; PLE map taken after 8 days of preparation
E	E1	D$_2$O	0.7	0.03		SDBS used as dispersant

[a] The estimated instrumental error is within $\pm 10\%$. [b] The final SWNT concentrations represent the average values calculated from absorption coefficients (α_λ) of SWNTs in NMP at 506, 660, 871, and 1308 nm and exclude 20 wt % impurities present in the SWNT sample.

(Sigma-Aldrich) by 1 h of ultrasonic treatment (Bioruptor; Diagenode) at 270 W, 20 kHz. After sonication, all the dispersions appear completely free from aggregates by visual inspection. The dispersions are immediately vacuum-filtered through binder-free glass fiber filters (Millipore and Sterlitech Corp.). Before sonication, group A is divided into three subgroups, containing ≈0.9 g/L nonionic surfactants (Igepal DM-970, Triton X-100, and Pluronic F98 in A1, A2, and A3, respectively). After ultrasonic treatment, groups A, C, and D are vacuum-filtered by 0.7 μm filters (retention diameter). Group B is divided into three subgroups, according to the nominal ratings of the filters used (0.7, 0.5, and 0.3 μm). After filtration, group C is divided into three 2.5 mL aliquots. To these we add 1.67, 3.33, and 6.67 g/L PVP (average molecular weight ≈29 000 Da; Sigma-Aldrich). All the nine samples in groups A, B, and C are used for the dispersion stability study over a period of 3 weeks. This length of observation is deemed to be sufficient to study the SWNT aggregation process by PL spectroscopy. After filtration, 5 g/L of PVP are added to a 2.5 mL portion of group D (D3). Two other 2.5 mL aliquots of the filtered dispersion are used for PLE measurements; just after preparation (D1) and after 8 days of incubation (D2). The incubation period for group D dispersions is also considered to be adequate to study the "debundling" and stabilization process.

After preparation, all the dispersions are sealed and kept at room temperature (21 °C) in a dark place. In addition to these four groups of SWNT/NMP dispersions, group E contains a single surfactant-aided and vacuum-filtered (0.7 μm) SWNT dispersion in D$_2$O (SWNT/D$_2$O). This is prepared using the same ultrasonic treatment as that of groups A, B, C, and D. Here, 1.4 g/L of sodium dodecylbenzene sulfonate (SDBS) is used to disperse 0.04 g/L (≈0.03 g/L without catalysts) of purified HiPco SWNTs in D$_2$O (Sigma-Aldrich). Note that, unlike what is often done in the literature,[12–16,27,32,34] none of the dispersions are centrifuged. Table 1 lists all the dispersions used in this study.

Photographic images of D1, C1, A2, and B2 dispersions in cuvettes after 3 weeks of preparation are shown in Figure 1. These dispersions represent the different SWNT concentrations we have studied here. Note that D1 appears darker than the other dispersions because of the higher SWNT concentration (see Table 1). With the same starting concentration of SWNTs, surfactant-assisted dispersion A2 appears darker than the dispersions in pure NMP (C1 and B2). Also, all the dispersions appear free from aggregates by visual inspection.
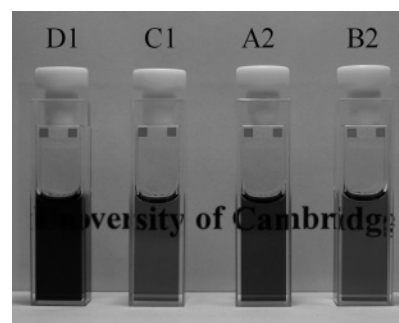

Figure 1. SWNT/NMP dispersions after 21 days of preparation. The dispersions remain completely aggregation-free by visual inspection. Note the difference in color due to difference in SWNT concentration (see Table 1).
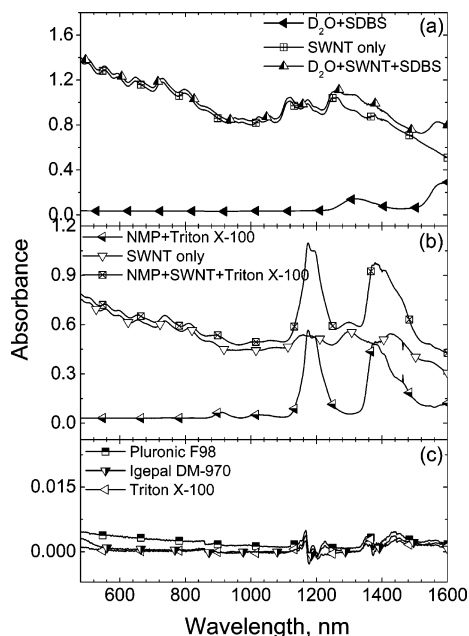
UV−vis absorptions of all the filtered dispersions are measured with a Perkin-Elmer Lambda 950 UV−vis spectrometer with 1.3 nm steps. All the absorption spectra are background subtracted, to account for solvent and surfactant, where appropriate (see Figure 3). PLE measurements are carried out in a HORIBA Jobin Yvon excitation−emission spectrofluorometer (Fluorolog-3) equipped with a xenon lamp excitation source and an InGaAs detector (Symphony solo) cooled by liquid nitrogen. The PL intensity measurements for the stability study are taken at 720 nm excitation, because the highest number of nanotube species in HiPco samples can be observed with this wavelength.[38,39] PLE maps are used to monitor nanotube "debundling" in group D dispersions. The maps are measured by scanning the excitation wavelength from 500 to 800 nm with 6 nm steps and 60 s exposure for an emission range from 1050 to 1350 nm. This window covers most of the SWNT species present in the HiPco samples.[40] The entrance and exit slit widths are 14 nm for all PL measurements.

3. Results and Discussion

Figure 2 shows the chemical structures of the three nonionic surfactants used in this study. Triton X-100 has been previously used for SWNT dispersions in water.[13,41−43] It has a short alkyl chain compared to the other two surfactants we consider here. However, its headgroup contains an aromatic ring, which is believed to interact effectively with the sidewalls of SWNTs in aqueous environments.[13,41] Igepal DM-970 is a long-chain surfactant reported to produce good dispersion of SWNTs in
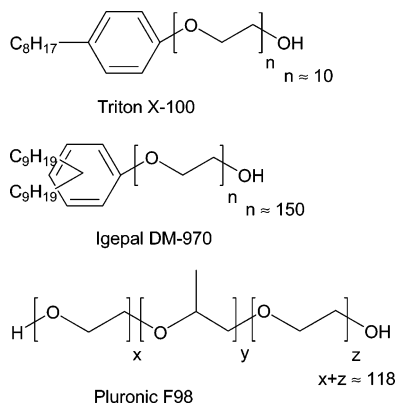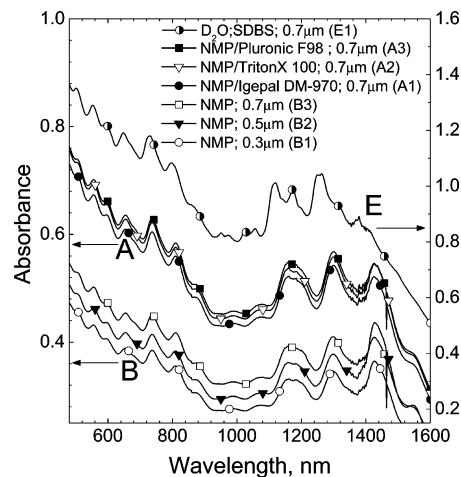
Figure 2. Chemical structures of the nonionic surfactants used in this study.

Figure 4. Absorption spectra of SWNTs in NMP (groups A and B) and D_2O dispersions. Note that background (solvent and surfactant, where appropriate) has been subtracted from all the spectra as shown in Figure 3.

Figure 3. Representative set of absorption spectra showing the absorbance peak positions of (a and b) solvent, surfactant, and SWNTs and (c) surfactants used in group A dispersions.

water. It also has an aromatic ring in its headgroup like Triton X-100. Pluronic F98 is a PEO−PPO−PEO[44] triblock polymer (average molecular weight $\approx 13\,000$ Da)[45] which was reported to be effective in SWNT dispersion in aqueous media.[15] The latter two surfactants are chosen to investigate the effect of their long chains (PEO chains in the case of Pluronic F98) for nanotube wrapping and solution stabilization through steric hindrance.[20,41]

A set of representative absorption spectra is presented in Figure 3. Figures 3a, 3b show the absorption spectra of "solvent + surfactant", "SWNT only", and "SWNT + solvent + surfactant" separately. In Figure 3b, the SWNT absorption band at ≈ 1200 nm coincides with an absorption peak of NMP and is therefore avoided for SWNT concentration calculations in latter sections of this article. Figure 3c shows absorption spectra of the nonionic surfactants used in this study. The oscillations at ≈ 1200 and 1400 nm arise from the sharp absorption peaks of NMP in which the surfactants are solvated for measurements. Clearly, absorption from surfactants is extremely low in the 500−1600 nm range. Nevertheless, the absorption from relevant surfactants has also been subtracted for group A dispersions. The absorption spectra in Figure 4 are similar to
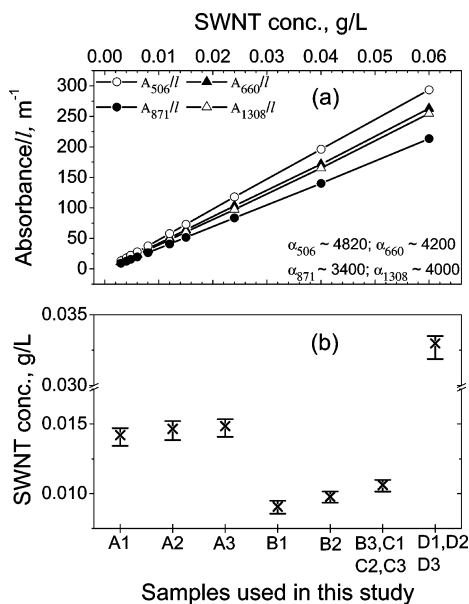
the "SWNT only" spectrum of Figure 3b, with appropriate background subtraction.

The absorption spectra of SWNTs in group A and B dispersions are shown in Figure 4. The absorption peaks at 1430 nm and beyond have a partial contribution from the moisture absorbed by NMP.[32,34] For comparison with SWNT/NMP dispersions, the absorption spectrum of the SWNT/D_2O dispersion (E1) is also presented. Well-resolved structures in the spectrum of E1 represent sharp interband transitions, indicating good dispersion and isolation of SWNTs even without centrifugation.[12,15] The other spectra from groups A and B show resolved structures indicating good dispersion too. However, the absorption peaks are red-shifted compared to E1. It is suggested that an increase in the electronic polarization dielectric constant (ϵ) of the surrounding environment causes a reduction in optical transition energies of SWNTs due to dielectric screening.[46−48] At optical frequencies, $\epsilon \approx n^2$ for most materials, where n is the refractive index at 589 nm (≈ 2.1 eV). The value of ϵ for D_2O and NMP are 1.764 and 2.16, respectively.[49] Also, the hydrophobic tail of the SDBS micelles surrounding the isolated SWNTs in an aqueous environment has a chemical structure similar to n-decane, whose ϵ is 1.993.[49] Therefore, the larger ϵ value of NMP than the hydrocarbon environment closely surrounding the SWNTs in SWNT/D_2O dispersions can induce a red-shift of the absorption peaks. In addition to dielectric screening, a reduction in optical transition energies was reported for bundled SWNTs compared to isolated ones.[46,50,51] Our SWNT/NMP dispersions should have a considerable amount of SWNT bundles due to our sample preparation method, not involving centrifugation. Therefore, due to dielectric screening and bundling, an overall reduction in optical transition energy and consequent red-shift is expected. We observe a 7 nm (≈ 25 meV) red-shift at 590 nm (≈ 2.1 eV) in the SWNT absorption spectrum in SWNT/NMP dispersions compared to SWNT/D_2O.

The absorption spectra of both groups A and B show a series of features from 400 to 550 nm (eh_{11} of metallic SWNTs, m-SWNTs), from 550 to 900 nm (eh_{22} of semiconducting SWNTs, s-SWNTs), and from 1100 to 1430 nm (eh_{11} of s-SWNTs).[12,30,31] The absorption peaks of groups A and B have very similar profiles. For example, the average full width at half-maximum (FWHM) of the ≈ 1300 nm band for group A and B dispersions is ≈ 51 nm (41 meV) and ≈ 47 nm (38 meV), respectively. They exhibit a broader profile for eh_{11} of s-SWNTs

Stabilization and "Debundling" of SWNTs in NMP

J. Phys. Chem. C, Vol. 111, No. 34, 2007 **12597**

Figure 5. (a) Beer–Lambert plot for absorption coefficient (α_λ) of HiPco SWNTs in NMP. The slope of the plots gives α_λ values. (b) Average values (cross) and error margins of the concentrations of the SWNT dispersions calculated from α_{506}, α_{660}, α_{871}, and α_{1308} values.

compared to the SWNT/D$_2$O dispersion (E1) prepared under the same condition (FWHM ≈ 38 nm; 31meV). However, compared to previous reports of ultracentrifuged SWNT dispersions in amide solvents,[28–32] the absorption peaks of our vacuum-filtered samples are markedly sharper, indicating superior dispersions.[50–52]

To estimate the SWNT concentration in the SWNT/NMP dispersions after vacuum filtration, the absorption coefficient (α) of HiPco SWNTs in NMP must be measured. For this purpose, SWNT dispersions with different known concentrations ranging from 0.06 to 0.003 g/L are prepared for absorption measurements by ultrasonic treatment without any centrifugation or vacuum filtration. Estimated instrumental error of the known SWNT concentrations is within ±7%. Absorption coefficients of HiPco SWNTs at four different wavelengths are measured using the Beer–Lambert law $A_\lambda = \alpha_\lambda l c$, where A_λ is the absorbance of the material at wavelength λ, α_λ is the absorption coefficient at wavelength λ, l is the length of the optical path, and c is the concentration of the material. The wavelengths are chosen to match well-defined peaks in the absorption spectra of SWNTs in NMP: eh_{11} of m-SWNTs (at 506 nm), eh_{22} of s-SWNTs (at 660 and 871 nm), and eh_{11} of s-SWNTs (at 1308 nm). Note that we consider negligible contribution from the catalysts present in the dispersion to absorption intensities at these wavelengths. Plots of A_λ/l at different wavelengths against SWNT concentrations (c) are shown in Figure 5a. The slope of the plots gives the values of α at different wavelengths (α_λ). In the observed SWNT concentration range, α_λ at any particular wavelength remains relatively constant, as evidenced from the slopes of the plots. The absorption coefficient for HiPco SWNTs in NMP at $\lambda = 660$ nm (α_{660}) was previously reported to vary between 3250 and 3500 L g^{-1} m^{-1} for a concentration range of 0.1–0.001 g/L.[34] The difference between our measurement ($\alpha_{660} \approx 4200$ L g^{-1} m^{-1}) and that of ref 34 is probably because we take into account the presence of 20 wt % impurities in our HiPco SWNT samples. Since the difference in starting concentration of SWNTs in groups A, B, C, and D is low, a single value of α for a particular wavelength can be used without significant error. Applying the Beer–Lambert law (with α_{506}

= 4820, $\alpha_{660} = 4200$, $\alpha_{871} = 3400$, and $\alpha_{1308} = 4000$ L g^{-1} m^{-1} and averaging the resultant SWNT concentrations), we obtain the estimated concentrations of SWNTs in the SWNT/NMP dispersions as shown in Table 1. The average concentrations are shown in Figure 5b. The uncertainty in the calculated SWNT concentrations using different α_λ is within ±6%.

Figure 4 shows that for the same starting concentration of SWNTs, nonionic surfactants (group A) disperse a larger amount of SWNTs in NMP compared to pure NMP (group B). Also, surfactant-aided dispersions (group A) have nearly identical SWNT concentrations after filtration. Therefore, for a low starting SWNT concentration, the surfactants disperse nearly equal amount of SWNTs in spite of marked differences in their chemical structures. The absorption spectra of group B have similar FWHMs compared to that of group A albeit with different absorption intensities. In addition, no discernible shifts in the absorption peaks between groups A and B are observed.

Semiconducting SWNTs have direct band gap. Therefore, PL from isolated s-SWNTs due to exciton recombination is expected.[38,39,54] The authors of ref 12 successfully isolated SWNTs in surfactant-aided aqueous dispersions, enabling experimental monitoring of the electronic properties of SWNTs through bulk PL measurements. Since the pioneering work of Bachilo et al.,[38] PLE is one of the most common techniques to monitor nanotube dispersions.[32,34,39,53] PLE also allows investigation of the presence of isolated or small bundles of SWNTs in a sample.[55] Therefore, variation of PL intensity over time can provide significant information regarding the stability and aggregation of SWNTs.[56,57]

In bundles, additional exciton relaxation channels exist between adjacent SWNTs.[55] Therefore, peak PL intensities are expected to change significantly when the bundle sizes change, conveying information on the SWNT aggregation state.[55–57] The stability of the SWNT/NMP dispersions is investigated by monitoring the PL intensities at an excitation wavelength of 720 nm over a period of 3 weeks. Peak PL intensities of (8,6) and (9,4) nanotubes at 720 nm excitation are plotted in Figure 6. The peak intensities are measured after subtraction of corresponding nonresonant baselines, as shown by the dashed lines for (9,4), (8,6), and (8,7) tubes in Figure 7.

The plots for (8,6) tubes in Figure 6A show that the dispersion aided by Pluronic F98 (A3) has a lower PL intensity compared to that of the other two surfactants (A1 and A2). The PL intensities of all the three solutions in group A decrease sharply during the first few days indicating microscopic aggregation of the dispersed nanotubes.[55,57] At the end of the third week, the emission intensities become stable and comparable to each other. After 2 months, visual inspection shows large aggregates in group A. Therefore, steric hindrance has little effect on SWNT/NMP stabilization unlike for SWNT dispersions in aqueous media.[15,17,20,41] In aqueous media, it was reported that the presence of aromatic rings in surfactant molecules affects the dispersion and stabilization of SWNTs, probably by π-like stacking on sidewalls.[13,41] However, the aromatic ring in the structure of Triton X-100 and Igepal DM-970 does not appear more advantageous than Pluronic F98 in terms of the total amount of SWNTs dispersed (see Table 1). The presence of the aromatic ring facilitates SWNT isolation, as suggested from the higher initial PL intensities of the Triton X-100 and Igepal DM-970 dispersions, Figure 6A. However, the SWNT aggregation process seems to be unaffected by the presence of the aromatic rings, as the PL intensities of group A become comparable to each other after 3 weeks. Therefore, we conclude that the aromatic ring in the surfactants promotes isolation of
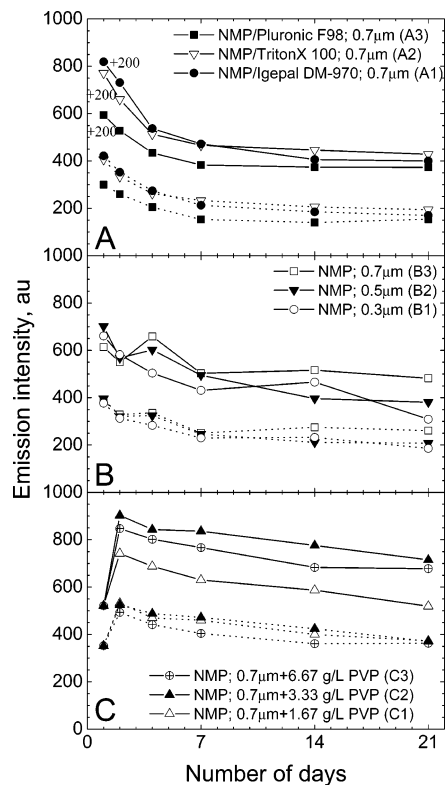
Figure 6. PL intensities of (8,6) species (solid lines) and (9,4) species (dashed lines) in group A, B, and C dispersions at 720 nm excitation wavelength over a period of 3 weeks. The increase in PL intensities of group C dispersions after the addition of PVP should be noted.
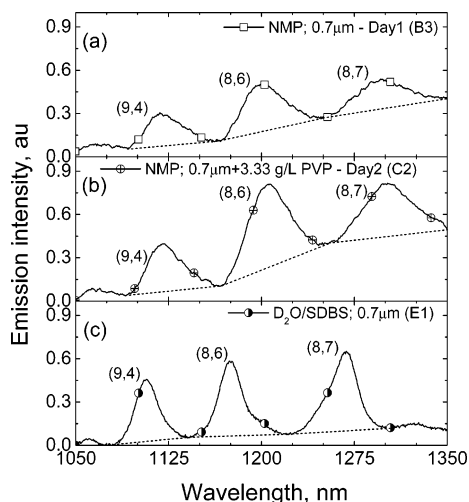
Figure 7. PL intensities of SWNT dispersions in NMP and D_2O at 720 nm excitation wavelength. Plots 7a and 7b have same exposure time and slit widths. The PL intensities increase significantly after 24 h of the addition of PVP (C2) to the SWNT/NMP dispersion (B3). PL intensity of E1 is shown to compare the peak positions but is not in scale with 7a,b. The dashed lines represent the baselines used to measure the peak intensities for Figure 6.

the SWNTs but is not the deciding factor for the amount of SWNTs dispersed in NMP or the stabilization of such dispersions.

Note that the number of surfactant molecules in group A are different because of their different molecular weights (molecular weight of Triton X-100, Igepal DM-970, and Pluronic F98 are ≈600−660, ≈7200, and ≈13 000 Da, respectively[45,58]). In a conservative estimation, if we assume the average length of SWNTs after the 1 h ultrasonication ≈500 nm, then, e.g., an

(8,6) nanotube of such length will weigh ≈700 kDa. Therefore, all the surfactant molecules in group A are present in excess numbers compared to the number of SWNTs. In terms of the total amount of SWNTs dispersed (as determined by UV−vis measurements), 0.9 g/L surfactants is found to be the commonly optimized concentration when 0.03 g/L SWNTs is used for ultrasonication in NMP. Small change in surfactant concentrations does not affect the dispersibility of SWNTs. However, UV−vis measurements show that a marked increase in the concentration of Igepal DM-970 and Pluronic F98 significantly reduces the total amount of SWNTs dispersed in NMP. For example, when the same molar concentration of Pluronic F98 and Igepal DM-970 are used compared to Triton X-100 in sample A2 (≈1.4 mmol/L), the estimated SWNT concentration in the solutions reduces to ~0.004 and ~0.0008 g/L, respectively. Note that error margin in the above estimation is expected to be higher at such small concentrations.

PL intensities of (8,6) tubes in NMP dispersions filtered by different filters (group B) also decrease over time. As seen in Figure 6B, a gradual decrease in the PL intensity of the (8,6) species is observed, similar to that observed in group A dispersions. The nominal rating of the filters (0.7, 0.5, and 0.3 μm) seems to have a negligible effect on solution stabilization. Thus, for low SWNT concentrations (≈0.010 g/L), the aggregation process is not very sensitive to submicrometer differences between SWNT bundle sizes. Like group A, group B dispersions also form visible aggregates after 2 months. Therefore, ultrasonicated and vacuum-filtered SWNT/NMP dispersions are not entirely thermodynamically stable even for a SWNT concentration as low as ≈0.010 g/L.

Nanotube aggregation in group B appears slower than group A in the first few days. Comparison shows that the reduction of the average PL intensities in groups A and B is 62% and 44%, respectively, 3 weeks after preparation. SWNT concentrations in group B are different from group A. Dispersions with higher SWNT concentrations aggregate faster because of the shorter mean distance between the nanotubes. Therefore, faster aggregation is expected in group A dispersions than group B. However, considering the large difference in PL intensity reduction in group A compared to group B, we conclude that, although the three nonionic surfactants produce better SWNT dispersions in NMP compared to pure NMP, they do not help in stabilizing the resulting solution.

PVP has been successfully used in aqueous micellar dispersions of SWNTs for "competitive" wrapping[12] and for direct SWNT dispersions.[14,36] In both cases, PVP is considered to wrap around the nanotubes to achieve better thermodynamic stability, eliminating the hydrophobic interface between the tubes and surrounding aqueous medium. Although the stabilization process of SWNTs in pure NMP is not completely understood,[34] we hypothesize that the introduction of PVP in SWNT/NMP dispersions might result in a "competitive" attachment process between PVP and NMP molecules and the SWNT sidewalls, similar to the effect observed between PVP molecules and surfactant micelles in aqueous SWNT dispersions.[12] To confirm this, additional PVP (1.67, 3.33, and 6.67 g/L) is added to the vacuum-filtered dispersions (group C). The PL intensities of the (8,6) tubes increase by as much as 73% after the first 24 h; see Figure 6C. Note that after PVP addition, these dispersions are not subjected to any external disturbance. In aqueous dispersions, PVP wrapping is governed by the removal of the hydrophobic interface between the SWNTs and water/D_2O, driven by thermodynamic stability.[14] Such a strong hydrophobic interface does not exist in the case of SWNTs dispersed in pure

Stabilization and "Debundling" of SWNTs in NMP

J. Phys. Chem. C, Vol. 111, No. 34, 2007 **12599**

NMP as NMP is much less polar than water.[49] Our experimental results indicate that SWNTs prefer PVP molecules to NMP, even though NMP was previously reported to disperse isolated SWNTs.[34] The reason for this preference is at present unclear. Group C dispersions are also found to aggregate over time, since the PL intensity decreases gradually. However, the rate of decrease in emission intensity is much slower than previous cases, indicating more stable dispersions. The addition of PVP changes the dielectric constant of the environment surrounding the SWNTs. Assuming that the dielectric constants of PVP ($\epsilon \approx 2.34$)[59] and NMP ($\epsilon \approx 2.16$)[49] measured at 590 nm (≈ 2.1 eV) maintain a similar difference between them at lower energies (e.g., at 1 eV), the change in surrounding environment is expected to slightly reduce the band gap of the SWNTs due to dielectric screening.[47,48] But, such a small shift will not modify the density of excitonic states and the exciton dynamics in nanotubes. However, "debundling" of nanotube aggregations can significantly improve the PL intensity of SWNT dispersions.[55] Therefore, we consider the increase in PL intensity of SWNT dispersions after the addition of PVP as a strong indication of spontaneous "debundling" of smaller SWNT aggregations triggered by PVP. This is further confirmed by the observation that no large aggregates can be visually detected in group C even after 4 months.

As shown in Figure 6C, the degraded PL intensity indicates that the wrapping of SWNTs with PVP molecules in NMP is not very strong. Therefore, it could be argued that in group A a larger number of excess surfactant molecules may be necessary to stabilize the SWNT dispersions. As discussed before, our experimental results with excess amount of Igepal DM-970 and Pluronic F98 in SWNT/NMP contradict this argument. By UV–vis measurements, the total amount of SWNTs dispersed is found to be significantly lower compared to samples A1 and A3. A similar effect on dispersion stability due to PVP concentration is observed in group C. Although the stability of these dispersions depends on PVP concentration, the plots for C2 and C3 in Figure 6C indicate that dispersion stability does not increase as the number of excess PVP molecules increases. Using the intensity increase and stability of the PL peak of the (8,6) species as reference, we find 3.33 g/L PVP (C2) to be more efficient than the other two (C1 and C3) in "debundling" and stabilizing the filtered dispersions.

The emission intensities of (9,4) tubes in groups A and B follow a similar pattern to (8,6), decreasing by approximately 50% after 3 weeks. A comparison between the (8,6) and (9,4) species in group C shows differences. The addition of PVP seems to have little impact on the stabilization of the (9,4) species. For example, 3 weeks after preparation, the peak intensity of (8,6) is 37% higher than the initial emission intensity in C2 dispersion. On the other hand, the (9,4) intensity is just 5% higher in the same dispersion. Furthermore, the emission intensities of (9,4) are not appreciably sensitive to the amount of PVP added. This suggests that the effect of PVP is preferential to certain nanotube species.

Figure 7 shows the PL emission profile of SWNTs in NMP and D_2O at 720 nm excitation. In comparison to the SWNT/D_2O dispersion (E1), the PL peak positions of (9,4), (8,6), and (8,7) tubes in pure NMP (B3) are red-shifted by ≈ 11.1, 20.4, and 19.9 meV (≈ 12, 26, and 27 nm), respectively. As discussed previously, this red-shift is caused by dielectric screening[46–48,54] and the presence of SWNT bundles.[46,50,51] Twenty-four hours after the addition of 3.33 g/L PVP to the SWNT/NMP dispersion (C2), the PL intensities of the (9,4), (8,6), and (8,7) species increase by 49%, 70%, and 82%, respectively, with correspond-

ing red-shifts of 2.3, 5.5, and 5.4 meV (2.8, 5 and 8.3 nm). The increase of PL intensities indicates "debundling". We think that the PVP molecules wrap around the SWNTs displacing NMP, thus increasing the ϵ of the environment surrounding the SWNTs. This results in a red-shift in optical transition energies of SWNTs. On the other hand, "debundling" of SWNTs is expected to cause a blue-shift in optical transition energy.[46] The overall effect determines the shift direction of the PL peaks. This is why a small red-shift in emission is observed, despite changes in dielectric environment. Varying amount of PL increase and corresponding peak shifts indicate that different SWNT species are probably being affected to different degrees by PVP. However, we find no strong correlation between change in emission intensities and corresponding shifts in the emission peak positions. In comparison to SWNT dispersions in pure NMP, the addition of PVP makes the PL peaks sharper, as shown in Figure 7. For example, the FWHM of the PL peak from the (8,7) species decreases by ≈ 2 nm (1.6 meV) after PVP addition. This further confirms "debundling" of SWNTs after addition of PVP accompanied by change in the surrounding dielectric environment.

The effect of PVP in "debundling" different SWNT species can be observed by comparing PLE maps from group D, which has a higher concentration of SWNTs (0.033 g/L) than groups A, B, and C (0.010–0.015 g/L). For stability studies, a higher concentration of SWNTs in dispersion has two advantages. First, a more concentrated dispersion will have shorter mean distances between the nanotubes, thereby accelerating the process of aggregation. Second, a large number of SWNTs are likely to be present in the dispersion as small bundles since no ultra-centrifugation is used. Therefore, the effect of "debundling" in group D will be more pronounced.
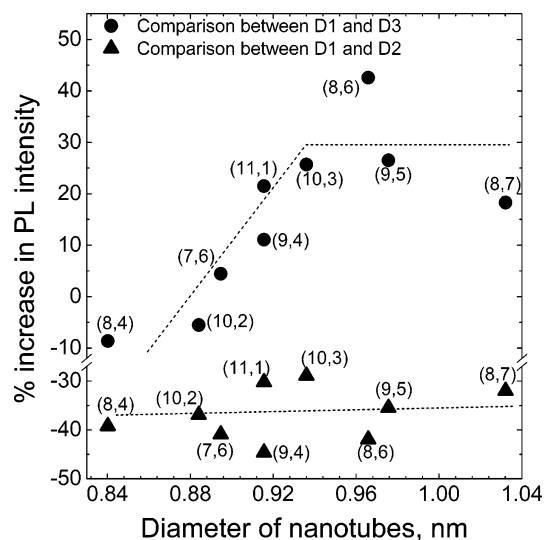
The PLE maps of three solutions (i.e., D1, D2, and D3) are obtained with an excitation range of 500–800 nm and an emission range of 1050–1350 nm, as shown in Figure 8. In comparison to previously reported HiPco SWNTs,[38,60] the map of D1 shows broader and red-shifted emission peaks. Dielectric screening is primarily responsible for the red-shifts in emission peak positions.[47,48] A similar red-shift of electronic transition energies of isolated SWNTs in pure NMP was recently reported.[34] Also, the presence of bundles in the dispersion is expected to contribute to the red-shift.[46,50,51] In comparison to D1, the PLE map of D2 shows broadened and red-shifted PL peaks with reduced PL intensities. This is a sign of formation of small bundles or aggregations, as discussed above. However, dispersion D2 appears aggregation-free by visual inspection. Though broader, the position of the emission peaks in map D2 matches that of ref 34. The most significant red-shift is observed for (8,6) tubes (≈ 10 nm; 8.54 meV), accompanied by a 42% decrease in PL intensity. The highest intensity decrease (45%) is observed for (9,4) tubes, whereas (10,3) are found to be more stable with a 29% decrease in corresponding intensity. The diameter of (9,4) and (10,3) is very similar, ≈ 0.92 and ≈ 0.94 nm, respectively. Therefore, it is unlikely that the aggregation process is diameter dependent. By comparing the PL intensities of each (*n,m*) species in maps D1 and D2 in Figure 8, no significant family dependence on the aggregation process is observed (Figure 9).

The PLE map of D3 shows a remarkable resemblance to the map of D1. This implies that after the addition of PVP, the SWNT dispersion remains stable. PL intensities of (8,4) and (10,2) species in D3 decrease by 8.6% and 5.5%, respectively, compared to D1. But the PL intensities of other species
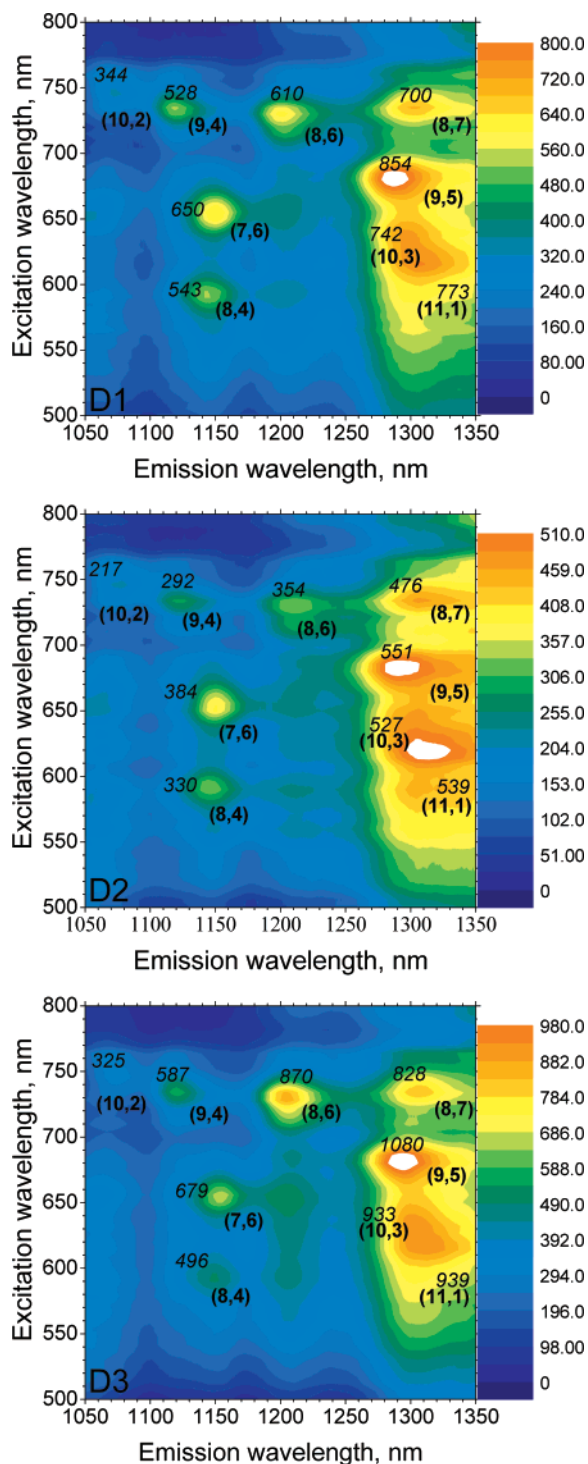
Figure 8. PLE maps showing the effect of PVP in stabilization of group D dispersions: map D1, as-prepared vacuum-filtered SWNT/NMP dispersion; maps D2 and D3, the same dispersion after 8 days of incubation. PVP is added immediately after preparation in the case of map D3. The peak intensities and (*n,m*) assignments are indicated. Note the scale of each PLE map.

Figure 9. Relation between SWNT diameter and change in PL intensity of group D dispersions (Figure 8) after 8 days of incubation. Dashed lines are guides to the eye.

significantly increase by dissimilar percentages. Such effects are not observed when ≈7 g/L of surfactant (i.e., higher number of surfactant molecules than PVP in group C owing to their lower molecular weights) are directly added to the vacuum-filtered SWNT dispersions in pure NMP. After PVP addition and subsequent incubation of 8 days, the highest increase (42%) in intensity is observed for the (8,6) species with a 4 nm (3.6 meV) red-shift. The maximum drop (9%) in emission intensity is observed for the (8,4) species with a 7 nm (6.7 meV) red-

shift. By comparing the PL intensities of each (*n,m*) in maps D1 and D3, the change in PL intensity is found to be related to SWNT diameter, as shown in Figure 9. The PVP-induced debundling appears to be more efficient for nanotubes with higher diameter. Also, an interesting family dependence can be extrapolated, with species belonging to different families behaving differently. For example, the (8,7), (9,5), (10,3), and (11,1) nanotubes from family $M = (n - m)\text{mod}3 = 1$ do not show any significant difference in the change in PL intensities. In contrast, the change in PL intensities in the (8,6), (9,4), and (10,2) species from family $M = (n - m)\text{mod}3 = -1$ are enhanced, moving toward the armchair direction. In this study, we only probed a narrow range of diameters. A broader range of diameters and chiralities should be investigated in order to confirm this diameter and family dependence.

It is unclear how the debundling process takes place without any external agitation. It is likely that SWNTs in NMP are stabilized and debundled by "competitive" attachment of SWNT sidewalls between PVP and NMP molecules. We believe this process to be highly dependent on the thermodynamic instability caused by the addition of PVP. In spite of the excess presence of PVP molecules, their wrapping of SWNTs dispersed in NMP is not very strong compared to that of the aqueous SWNT dispersions, where excess PVP molecules could be extracted without destabilizing the dispersion.[14] The relatively weaker association between PVP−SWNT in NMP is evident from the slow but gradual degradation of PL signals in group C, see Figure 6C. Indeed, even ultracentrifuged surfactant-aided aqueous SWNT dispersions are reported to exhibit signs of nanotube aggregations over longer periods.[55] Preferential debundling and wrapping of larger diameter SWNTs is probably because of significant bond angle strains in the polymer backbone when PVP molecules try to wrap around smaller diameter SWNTs.[14] We find no evidence of spontaneous debundling when PVP and SWNTs are simply added to pure NMP, even after 2 weeks at 80 °C, as when SWNTs are directly added to NMP and subjected to similar treatment. Therefore, the spontaneous wrapping of nanotubes only takes place in the presence of very small aggregations or small bundles where the net van der Waals forces of attraction acting on SWNTs lying on the outer surface of the bundles are smaller.

Stabilization and "Debundling" of SWNTs in NMP

J. Phys. Chem. C, Vol. 111, No. 34, 2007 **12601**

4. Conclusions

We demonstrated that HiPco SWNT dispersions in pure NMP can be stabilized by adding PVP. The resulting solutions are found to be stable even after 3 weeks of incubation. After PVP addition, a significant increase in PL emission without any ultrasonic treatment strongly points to spontaneous debundling of small aggregates. At the same time, the relationship between increase in PL intensity and tube diameter shows that the debundling process is diameter sensitive and is more efficient for larger diameters. We also show that ultrasonicated and vacuum-filtered SWNT dispersions in NMP are not completely stable, even at low concentrations ($\approx$0.01 g/L). The as-prepared dispersions show PL emission, indicating a significant population of isolated SWNTs as well as small bundles. Three different nonionic surfactants are found to have little or no effect in SWNT/NMP dispersion stabilization. Surfactants, however, are found to disperse a higher amount of nanotubes compared to pure NMP. Our work opens the possibility of preparing PVP-aided high-quality dispersions of SWNTs in NMP in a two-step process, without significant functionalization. Consequently, high-quality optical or electronic-grade composites with a wide range of compatible polymers in a minimum number of steps could be possible.

References and Notes

(1) Thess, A.; Lee, R.; Nikolaev, P.; Dai, H.; Petit, P.; Robert, J.; Xu, C.; Lee, Y. H.; Kim, S. G.; Rinzler, A. G.; Colbert, D. T.; Scuseria, G. E.; Tománek, D.; Fischer, J. E.; Smalley, R. E. *Science* **1996**, *273*, 483.

(2) Journet, C.; Maser, W. K.; Bernier, P.; Loiseau, A.; Lamy de la Chapelle, M.; Lefrant, S.; Deniard, P.; Lee, R.; Fischer, J. E. *Nature* **1997**, *388*, 756.

(3) Girifalco, L. A.; Hodak, M.; Lee, R. S. *Phys. Rev. B* **2000**, *62*, 13104.

(4) Hertel, T.; Walkup, R. E.; Avouris, Ph. *Phys. Rev. B* **1998**, *58*, 13870.

(5) Charlier, J.-C.; Lambin, Ph.; Ebbesen, T. W. *Phys. Rev. B* **1996**, *54*, R8377.

(6) Coleman, J. N.; Khan, U.; Gun'ko, Y. K. *Adv. Mater.* **2006**, *18*, 689.

(7) Berber, S.; Kwon, Y.-K.; Tománek, D. *Phys. Rev. Lett.* **2000**, *84*, 4613.

(8) Kwon, Y.-K.; Saito, S.; Tománek, D. *Phys. Rev. B* **1998**, *58*, R13314.

(9) Dalton, A. B.; Collins, S.; Muñoz, E.; Razal, J. M.; Ebron, V. H.; Ferraris, J. P.; Coleman, J. N.; Kim, B. G.; Baughman, R. H. *Nature* **2003**, *423*, 703.

(10) Li, Y.-L.; Kinloch, I. A.; Windle, A. H. *Science* **2004**, *304*, 276.

(11) Liu, J.; Rinzler, A. G.; Dai, H.; Hafner, J. H.; Bradley, R. K.; Boul, P. J.; Lu, A.; Iverson, T.; Shelimov, K.; Huffman, C. B.; Rodriguez-Macias, F.; Shon, Y.-S.; Lee, T. R.; Colbert, D. T.; Smalley, R. E. *Science* **1998**, *280*, 1253.

(12) O'Connell, M. J.; Bachilo, S. M.; Huffman, C. B.; Moore, V. C.; Strano, M. S.; Haroz, E. H.; Rialon, K. L.; Boul, P. J.; Noon, W. H.; Kittrell, C.; Ma, J.; Hauge, R. H.; Weisman, R. B.; Smalley, R. E. *Science* **2002**, *297*, 593.

(13) Islam, M. F.; Rojas, E.; Bergey, D. M.; Johnson, A. T.; Yodh, A. G. *Nano Lett.* **2003**, *3*, 269.

(14) O'Connell, M. J.; Boul, P.; Ericson, L. M.; Huffman, C.; Wang, Y.; Haroz, E.; Kuper, C.; Tour, J.; Ausman, K. D.; Smalley, R. E. *Chem. Phys. Lett.* **2001**, *342*, 265.

(15) Moore, V. C.; Strano, M. S.; Haroz, E. H.; Hauge, R. H.; Smalley, R. E. *Nano Lett.* **2003**, *3*, 1379.

(16) Zheng, M.; Jagota, A.; Semke, E. D.; Diner, B. A.; Mclean, R. S.; Lustig, S. R.; Richardson, R. E.; Tassi, N. G. *Nat. Mater.* **2003**, *2*, 338.

(17) Hirsch, A. *Angew. Chem., Int. Ed.* **2002**, *41*, 1853.

(18) Yudasaka, M.; Zhang, M.; Jabs, C.; Iijima, S. *Appl. Phys. A* **2000**, *71*, 449.

(19) Star, A.; Stoddart, J. F.; Steuerman, D.; Diehl, M.; Boukai, A.; Wong, E. W.; Yang, X.; Chung, S.-W.; Choi, H.; Heath, J. R. *Angew. Chem., Int. Ed.* **2001**, *40*, 1721.

(20) Vaisman, L.; Marom, G.; Wagner, H. D. *Adv. Funct. Mater.* **2006**, *16*, 357.

(21) Chen, J.; Liu, H.; Weimer, W. A.; Halls, M. D.; Waldeck, D. H.; Walker, G. C. *J. Am. Chem. Soc.* **2002**, *124*, 9034.

(22) Wise, K. E.; Park, C.; Siochi, E. J.; Harrison, J. S. *Chem. Phys. Lett.* **2004**, *391*, 207.

(23) Lin, Y.; Taylor, S.; Li, H.; Fernando, K. A. S.; Qu, L.; Wang, W.; Gu, L.; Zhou, B.; Sun, Y.-P. *J. Mater. Chem.* **2004**, *14*, 527.

(24) Yu, A.; Hu, H.; Bekyarova, E.; Itkis, M. E.; Gao, J.; Zhao, B.; Haddon, R. C. *Compos. Sci. Technol.* **2006**, *66*, 1187.

(25) Niyogi, S.; Hamon, M. A.; Hu, H.; Zhao, B.; Bhowmik, P.; Sen, R.; Itkis, M. E.; Haddon, R. C. *Acc. Chem. Res.* **2002**, *35*, 1105.

(26) Georgakilas, V.; Kordatos, K.; Prato, M.; Guldi, D. M.; Holzinger, M.; Hirsch, A. *J. Am. Chem. Soc.* **2002**, *124*, 760.

(27) Liu, J.; Casavant, M. J.; Cox, M.; Walters, D. A.; Boul, P.; Lu, W.; Rimberg, A. J.; Smith, K. A.; Colbert, D. T.; Smalley, R. E. *Chem. Phys. Lett.* **1999**, *303*, 125.

(28) Ausman, K. D.; Piner, R.; Lourie, O.; Ruoff, R. S.; Korobov, M. *J. Phys. Chem. B* **2000**, *104*, 8911.

(29) Bahr, J. L.; Mickelson, E. T.; Bronikowski, M. J.; Smalley, R. E.; Tour, J. M. *Chem. Commun.* **2001**, 193.

(30) Landi, B. J.; Ruf, H. J.; Worman, J. J.; Raffaelle, R. P. *J. Phys. Chem. B* **2004**, *108*, 17089.

(31) Krupke, R.; Hennrich, F.; Hampe, O.; Kappes, M. M. *J. Phys. Chem. B* **2003**, *107*, 5667.

(32) Maeda, Y.; Kimura, S-i.; Hirashima, Y.; Kanda, M.; Lian, Y.; Wakahara, T.; Akasaka, T.; Hasegawa, T.; Tokumoto, H.; Shimizu, T.; Kataura, H.; Miyauchi, Y.; Maruyama, S.; Kobayashi, K.; Nagase, S. *J. Phys. Chem. B* **2004**, *108*, 18395.

(33) Furtado, C. A.; Kim, U. J.; Gutierrez, H. R.; Pan, L.; Dickey, E. C.; Eklund, P. C. *J. Am. Chem. Soc.* **2004**, *126*, 6095.

(34) Giordani, S.; Bergin, S. D.; Nicolosi, V.; Lebedkin, S.; Kappes, M. M.; Blau, W. J.; Coleman, J. N. *J. Phys. Chem. B* **2006**, *110*, 15708.

(35) Marcus, Y. *Chem. Soc. Rev.* **1993**, *22*, 409.

(36) Zhang, X.; Liu, T.; Sreekumar, T. V.; Kumar, S.; Moore, V. C.; Hauge, R. H.; Smalley, R. E. *Nano Lett.* **2003**, *3*, 1285.

(37) Nikolaev, P.; Bronikowski, M. J.; Bradley, R. K.; Rohmund, F.; Colbert, D. T.; Smith, K. A.; Smalley, R. E. *Chem. Phys. Lett.* **1999**, *313*, 91.

(38) Bachilo, S. M.; Strano, M. S.; Kittrell, C.; Hauge, R. H.; Smalley, R. E.; Weisman, R. B. *Science* **2002**, *298*, 2361.

(39) Bachilo, S. M.; Balzano, L.; Herrera, J. E.; Pompeo, F.; Resasco, D. E.; Weisman, R. B. *J. Am. Chem. Soc.* **2003**, *125*, 11186.

(40) Oyama, Y.; Saito, R.; Sato, K.; Jiang, J.; Samsonidze, Ge. G.; Grüneis, A.; Miyauchi, Y.; Maruyama, S.; Jorio, A.; Dresselhaus, G.; Dresselhaus, M. S. *Carbon* **2006**, *44*, 873.

(41) Tan, Y.; Resasco, D. E. *J. Phys. Chem. B* **2005**, *109*, 14454.

(42) Riggs, J. E.; Walker, D. B.; Carroll, D. L.; Sun, Y.-P. *J. Phys. Chem. B* **2000**, *104*, 7071.

(43) Rinzler, A. G.; Liu, J.; Dai, H.; Nikolaev, P.; Huffman, C. B.; Rodríguez-Macías, F. J.; Boul, P. J.; Lu, A. H.; Heymann, D.; Colbert, D. T.; Lee, R. S.; Fischer, J. E.; Rao, A. M.; Eklund, P. C.; Smalley, R. E. *Appl. Phys. A* **1998**, *67*, 29.

(44) PEO: polyethylene oxide. PPO: poly(*p*-phenylene oxide).

(45) More details on Pluronic F98 can be obtained from BASF.

(46) Wang, F.; Sfeir, M. Y.; Huang, L.; Huang, X. M. H.; Wu, Y.; Kim, J.; Hone, J.; O'Brien, S.; Brus. L. E.; Heinz, T. F. *Phys. Rev. Lett.* **2006**, *96*, 167401.

(47) Walsh, A. G.; Vamivakas, A. N.; Yin, Y.; Ünlü, M. S.; Goldberg, B. B.; Swan, A. K.; Cronin, S. B. *Nano Lett.* **2007**, *7*, 1485.

(48) Capaz, R. B.; Spataru, C. D.; Ismail-Beigi, S.; Louie, S. G. *Phys. Rev. B* **2006**, *74*, 121401(R).

(49) Riddik, J. A.; Bunger, W. B.; Sakano, T. K. In *Organic Solvents, Physical Properties and Methods of Purification*, 4th ed.; John Wiley & Sons, Inc.: New York, 1986; pp 129 and 666.

(50) Reich, S.; Thomsen, C.; Ordejón, P. *Phys. Rev. B* **2002**, *65*, 155411.

(51) O'Connell, M. J.; Sivaram, S.; Doorn, S. K. *Phys. Rev. B* **2004**, *69*, 235415.

(52) Dresselhaus, M. S.; Eklund, P. C. *Adv. Phys.* **2000**, *49*, 705.

(53) Iakoubovskii, K.; Minami, N.; Kazaoui, S.; Ueno, T.; Miyata, Y.; Yanagi, K.; Kataura, H.; Ohshima, S.; Saito, T. *J. Phys. Chem. B* **2006**, *110*, 17420.

(54) Lefebvre, J.; Fraser, J. M.; Homma, Y.; Finnie, P. *Appl. Phys. A* **2004**, *78*, 1107.

(55) Tan, P. H.; Rozhin, A. G.; Hasan, T.; Hu, P.; Scardaci, V.; Milne, W. I.; Ferrari, A. C. *Cond-Mat.* [Online] **2007**, 0704.2303v1; *Phys. Rev. Lett.* (in press, 2007).

(56) McDonald, T. J.; Engtrakul, C.; Jones, M.; Rumbles, G.; Heben, M. J. *J. Phys. Chem. B* **2006**, *110*, 25339.

(57) Niyogi, S.; Boukhalfa, S.; Chikkannanavar, S. B.; Mcdonald, T. J.; Heben, M. J.; Doorn, S. K. *J. Am. Chem. Soc.* **2007**, *129*, 1898.

(58) Obtained from the product information sheets from Sigma-Aldrich.

(59) Takahagi, T.; Saiki, A.; Sakaue, H.; Shingubara, S. *Jpn. J. Appl. Phys.* **2003**, *42*, 157.

(60) Weisman, R. B.; Bachilo, S. M. *Nano Lett.* **2003**, *3*, 1235.